Tolerance at the genetic level of the brine shrimp *Artemia salina* to a wide range of salinity

JunMo Lee
Kyungpook National University
Jong Soo Park (jongsoopark@knu.ac.kr)
Kyungpook National University https://orcid.org/0000-0001-6253-5199

Research

Keywords: Artemia salina, crustacean, differential expressed genes, euryhaline, halotolerant, transcriptome, osmoregulation

Posted Date: October 13th, 2020

DOI: https://doi.org/10.21203/rs.3.rs-91049/v1

Abstract

Background: The brine shrimp *Artemia salina* can thrive in a variety of salinities and is commonly distributed in natural hypersaline lakes and solar salterns. The zooplankter *A. salina* proves to be a filter feeder, consuming the alga *Dunaliella* and prokaryotes and plays a critical role in the hypersaline food web. However, the high salinity adaptation mechanisms of *A. salina* remain poorly understood through transcriptome analysis. Here, we examined the gene expression patterns of *A. salina* adults that were salt-adapted for 2–4 weeks at five salinities (35, 50, 100, 150, and 230 psu), and generated long-read isoform sequencing (IsoSeq) data to construct a high-quality transcriptome assembly of *A. salina*. The patterns of *A. salina* along the salinity gradient provide evidence for halotolerant and euryhaline adaptations at the genetic level.

Results: We confirmed that the activity of sodium/potassium ATPase was up-regulated at the genetic level in high salinity waters. Interestingly, genes related to beta-mannosidase and mannose activities were also up-regulated, suggesting that mannose and mannose derivatives may be accumulated as organic osmolytes. Alternatively, considering that glucose and galactose-related activities were suppressed at high salinities, mannose may be the primary sugar involved in the glycolytic pathway under such conditions. This result further supports the theory that mannose is the main energy source used by *A. salina* in highly saline environments. The gene expression patterns of *A. salina* may also be affected by increased thickness of the cuticle, increased numbers of mitochondria, and low dissolved oxygen in high salinity waters. Furthermore, the cellular response of *A. salina* to acclimation to intermediate salinities depends on the number and type of genes expressed; differential expression patterns are likely to fluctuate at the population level.

Conclusions: Our results provide a high-quality transcriptome assembly of the cosmopolitan brine shrimp *Artemia salina* at five different salinities (35, 50, 100, 150, and 230 psu) for the first time. The gene expression patterns of salt-adapted *A. salina* display greater osmoregulation process complexity than we thought. Furthermore, *A. salina* represents a potential model organism to study locally adapted populations at various salinities.

Background

Hypersaline environments have existed on Earth since before the Cambrian period, providing extraordinary habitats for all domains of life [1]. Prokaryotes are the most abundant life forms in extreme saline environments, whereas eukaryotes rarely inhabit them [2–4]. Previously, a simplified grazing food chain was proposed for hypersaline environments [3]: phytoplankton (*Dunaliella*) → zooplankton (*Artemia*). More recently, however, several halotolerant and halophilic protozoa have been reported or re-described in these environments, revealing a more complex food chain than previously understood [4–16]. Regardless of those reports, the zooplankter *Artemia salina* is undoubtedly a predominant part of the food chain in high salinity waters that transfers energy to higher trophic levels (e.g., birds) around hypersaline environments worldwide [3, 17].

The brine shrimp *A. salina* (Branchiopoda; Pancrustacea; Crustacea) is often observed in natural hypersaline lakes (e.g., the Great Salt Lake) as well as in artificial solar salterns [18, 19]. This zooplankter can survive in saline waters ranging from 5 psu (practical salinity unit) to > 300 psu, demonstrating that it is a halotolerant and euryhaline species [20–22]. *A. salina* is a filter feeder, consuming phytoplankton (e.g., *Dunaliella*) and prokaryotes in these high salinity waters. Thus, this extremophile species must be a strict osmoregulator, as it regularly ingests high salinity water along with prey [23–26]. Several studies report that an increase in salinity stimulates Na^+ /K^+-ATPase activity in multiple organs (e.g., metepipodites, maxillary glands, and gut) of adult *A. salina* for the excretion of accumulated salts [23–26]. In addition, the hemolymph of *A. salina* is maintained at a constant ~ 300 mOsm/kg (9 psu salinity), which is similar to the osmolality of teleost fishes, when exposed to a range of external high salinities [25, 27]. However, the differential gene expression patterns in adult *A. salina* along salinity gradients have not been investigated [22]. Moreover, other adaptive osmoregulatory mechanisms of *A. salina* to differing salinity ranges remain poorly understood.

Here, we generated a *de novo* transcriptome assembly of adult *A. salina* using a hybrid assembly approach, with long-read isoform sequencing and high-throughput RNA sequencing data, to analyze the differential gene expression patterns in a variety of salinities (i.e., 35, 50, 100, 150, and 230 psu). In the present study, *A. salina* significantly up-regulated genes (e.g., Na^+/K^+-ATPase gene) related to osmoregulation with increasing salinity from 35 psu to 230 psu. In addition, we note that low oxygen concentration and thickness of *A. salina*'s body surface may greatly affect its metabolic processes at high salinities.

Methods

Sample preparation, isoform, and RNA sequencing of Artemia salina

Artemia salina was isolated from 140 psu saline water collected from a solar saltern in Uiseong (36°60'20.86"N, 126°29'71.16"E), Republic of Korea, in April 2018 (Fig. 1; an additional movie file shows this in more detail [see Additional File 1]). A population of male and female *A. salina* in a 20-L aquarium, also containing sediment from the saltern and 15 L artificial saline water made by dilution of Medium V (300 psu) [28], was maintained at 150 psu. Approximately 20 adults with a half-and-half sex ratio were transferred and maintained in artificial saline water at 35, 50, 100, 150, and 230 psu for 2–4 weeks. After this time, we collected 10 adults (five males and five females) from each salinity medium to perform transcriptome-level analyses of isoforms. Total RNA was extracted from *A. salina* using the RNeasy Plus Mini Kit (Qiagen, Hilden, Germany). The RNA sequencing libraries were constructed using the Illumina Truseq Standard mRNA Prep Kit (Illumina Inc., San Diego, CA, USA), and the qualities of the libraries were checked using a 2100 Bioanalyzer (Agilent Technologies, Santa Clara, CA, USA). The RNA sequencing libraries were sequenced using 100-bp paired-end reagents with an Illumina Novaseq6000 (Table S1 in Additional File 2). The isoform sequencing (IsoSeq) library was constructed using a SMARTer PCR cDNA Synthesis Kit and DNA Template Prep Kit 1.0; the IsoSeq data were generated (1.0 Gbp; 780,667 reads) using the PacBio Sequel platform (Pacific Biosciences, Menlo Park, CA, USA). The high-quality (HQ)

isoform consensus (16.6 Mbp; 16,555 reads) of the IsoSeq data was constructed using a SMRT Link 5.1.0 with the Iso-Seq2 application platform. Raw reads of RNA sequencing and high-quality Isoform consensus data were uploaded to the NCBI SRA (Sequence Read Archive) database with accession numbers (SRR12358297 – SRR12358302; BioProject PRJNA649341).

De novo **transcriptome assembly, protein predictions, and functional annotations**

To construct high-quality isoform sequences, we generated a hybrid *de novo* transcriptome assembly of *Artemia salina* using a long-read HQ isoform consensus (16.6 Mbp; 16,555 reads; PacBio Sequel) and high-throughput RNA sequencing (a total of 34.6 Gbp; 100 × 100 bp Illumina Novaseq6000 reads). To improve sequence accuracy, the error correction step of the IsoSeq consensus was performed using the high-accuracy Illumina sequencing reads, which were aligned by Bowtie2, and variant calling in the alignment was processed using the Samtools program (Figure S1 in Additional File 3) [29, 30]. The corrected IsoSeq reads were assembled with the short-read Illumina sequencing data using the Trinity assembler (v2.8.4; default option of *de novo* transcriptome assembly with '–long_reads') [31, 32]. To reduce redundancy, the assembled transcripts were clustered using the cd-hit-EST program (v4.6; -c 0.95 -aS 0.95 -n 10; https://github.com/weizhongli/cdhit). The RNA-seq raw reads were mapped into the assembled transcripts using the Salmon program (default options) [33], and the potential false-positive transcripts including zero-tpm (transcripts per million) values were excluded. Potential ribosomal RNA fragments in the assembled transcripts were excluded based on the results of a local BLASTn search (*e*-value cutoff = 1.e-10) using *Artemia salina* ribosomal RNA sequences (X01723.1 and AF169697.1).

All possible open reading frames (ORFs) in the assembled transcriptome data were predicted by a 6-frame translation by Python (minimum length of protein-coding sequences = 150 bp), so that all three forward and reverse transcript frames were translated with the standard code (NCBI genetic code table 1). From the predicted ORFs, only homologous pancrustacean proteins were selected for downstream analysis, based on the results of a local BLASTp search (*e*-value cutoff = 1.e-05). The reference protein database for the BLASTp search was constructed from pancrustacean species as follows: *Armadillidium nasatum* (NCBI, SEYY00000000.1), *Artemia franciscana* (https://antagen.kopri.re.kr/), *Catajapyx aquilonaris* (BCM-HGSC; https://i5k.nal.usda.gov), *Daphnia magna* (NCBI, QYSF00000000.1), *Daphnia pulex* (NCBI, FLTH00000000.2), *Eulimnadia texana* (NCBI, NKDA00000000.1), *Eurytemora affinis* (NCBI, AZAI00000000.2), *Folsomia candida* (NCBI, LNIX00000000.1), *Lepidurus arcticus* (NCBI, RJJB00000000.1), *Lepidurus apus lubbocki* (RJJA00000000.1), *Orchesella cincta* (NCBI, LJIJ00000000.1), *Penaeus vannamei* (NCBI, NIUR000000000.1), *Tigriopus californicus* (NCBI, VCGU00000000.1), *Tribolium castaneum* (NCBI, AAJJ00000000.2), and *Zootermopsis nevadensis* (NCBI, AUST00000000.1) [34–45]. The predicted proteins and their coding sequences are available in Additional File 4. Functional annotations of the predicted proteins from the assembled transcriptome of *A. salina* were carried out using eggNOG-mapper [46] and KEGG blast (http://www.genome.jp/tools/blast/).

Analyses of conserved eukaryotic gene sets and phylogeny

Conserved eukaryotic gene set completeness analyses were conducted using BUSCO (Benchmarking Universal Single-Copy Orthologs; v3.0.2) [47, 48]. Sixteen taxa from Pancrustacea, including *A. salina*, were used to reconstruct the molecular phylogenetic tree. The phylogenetic position of *A. salina* was inferred using 5,604 concatenated protein sequences, which were related to Pancrustacea (local BLASTp *e*-value cutoff = 1.e-05). All protein sequences were aligned using MAFFT v7.313 (default options: –auto) [49]. Each alignment was trimmed when an aligned locus included more than 70% gap sequences. The phylogenetic analysis was inferred using maximum likelihood (ML) analysis. The ML tree was estimated using IQ-tree v.1.6.12 [50] with the best-fit evolutionary model, and statistical support was estimated using bootstrapping with 1,000 replicates.

Differentially expressed gene analysis of Artemia salina

Mapping of RNA-seq raw reads was performed using Salmon (default option) [33] for differentially expressed gene (DEG) analyses of *A. salina* at 35, 50, 100, 150, and 230 psu. The tpm (transcripts per million) values were normalized by the z-score [('Expression' - 'Average expression of all conditions in each gene') / 'Standard deviation of all conditions in each gene']. Based on the z-score dynamics of each gene candidate, we analyzed up- and down-regulated gene expression patterns using customized Python scripts, and sorted the genes by salinity-dependent gene expression patterns including only those with following criteria: maximum fold-change ≥ 2-fold between the highest and the lowest tpm value, and the lowest tpm ≥ 5 in a target gene. Gene ontology (GO) terms were extracted from the functional annotations of the target genes described by the eggNOG-mapper results, and the enrichment of GO terms was performed using the topGO package in R (Fisher test, *p*-value < 0.05).

Results

De novo **transcriptome assembly and phylogenomic analysis**

A total of 18,301 protein-coding sequences from *Artemia salina* were obtained through filtration of the assembled transcripts (i.e., removing too-short, redundant, and false-positive transcripts). Reference data were used for the homologous pancrustacean sequences (Figure S1 in Additional File 3; see above). Based on the BUSCO analysis, the protein profiles of *A. salina* included 92.3% conserved eukaryotic gene sets, a reliability quality comparable to those of other crustaceans (85–94% of BUSCOs; Table S2 in Additional File 2). The class Branchiopoda, which includes *A. salina*, formed a robust clade, and *A. salina* was closest to *A. franciscana* with maximal bootstrap support (ML: 100%; Fig. 2). Branchiopoda was the sister group to the class Hexapoda (ML: 100%), which also formed a monophyletic group (Fig. 2).

Differentially expressed gene patterns along the salinity gradient

Due to the wide salinity tolerance range of *A. salina*, we evaluated variations in the gene expression patterns of salt-adapted cells along a salinity gradient (35 psu to 230 psu) based on z-scores using

custom Python scripts (Python v2.7.16; Fig. 3). The enriched GO terms of the salinity-dependent genes (topGO package in R, Fisher test, *p*-value < 0.05) revealed that *A. salina* significantly up-regulated genes related to Na^+/K^+-ATPases, mannose and carotenoid metabolism, and monocarboxylate transmembrane transporters with an increase in salinity from 35 psu to 230 psu (Fig. 3; Table S3 and S4 in Additional File 2; Figure S2 in Additional File 3). Conversely, *A. salina* significantly down-regulated genes associated with galactose, and glucose metabolism, N-acetylgalactosamine-4-sulfatases, amino acid symporters, and amino acid transmembrane transporters in a salinity-dependent trend (Fig. 3; Table S3, and S4 in Additional File 2; Figure S2 in Additional File 3). Interestingly, the frequency of acidic, basic, hydrophilic, and hydrophobic amino acids in *A. salina* was identical to that of other pancrustacean species (Table S5 in Additional File 2). This result suggests that the osmoregulation system of the extremely euryhaline *A. salina* may operate by excreting excess salts instead of involving conformational changes to the proteomes within the animal's cells.

In addition to the those involving osmoregulatory processes of *A. salina* (e.g., Na^+/K^+-ATPase), transcripts related to the visual cycle and mitochondrial morphogenesis were also up-regulated in hypertonic waters (Fig. 3; Table S4 in Additional File 2). Furthermore, genes involved in oxidative stress regulation and glycoprotein catabolic processes were up-regulated at high salinities (Fig. 3; Table S4 in Additional File 2). In contrast, the transcript encoding N-acetylgalactosamine-4-sulfatase, which hydrolyzes sulfates, was down-regulated in high salinity waters (Fig. 3; Table S4 in Additional File 2). Furthermore, *A. salina* noticeably down-regulated genes related to diverse transporter activities in response to high salinity (Fig. 3; Table S4 in Additional File 2). This indicates that the transporter systems in adult *A. salina* may be repressed in highly saline environments.

U-shaped or inverted U-shaped expression patterns

Artemia spp. grow best in a salinity range of 100–150 psu and can tolerate < 5 psu or > 300 psu [20–22, 51, 52]. Therefore, some genes may be expressed in a quadratic profile, such as a U-shaped (i.e., up-regulated at the two salinity extremes) or inverted U-shaped (i.e., down-regulated at the two salinity extremes) curve. A total of 326 *A. salina* genes were expressed in U-shaped curves with the lowest point at 50 psu; 222 and 411 genes were expressed in U-shaped curves with the lowest points at 100 and 150 psu, respectively (Fig. 4; Table S6 in Additional File 2). Furthermore, inverted U-shaped expression patterns were observed in 379 genes with the highest point at 50 psu; 289 and 63 genes were detected with the highest points at 100 and 150 psu, respectively (Fig. 4; Table S6 in Additional File 2).

Several studies report that selected *Artemia* genes were up-regulated or down-regulated in response to high salinity [22, 53–58]. Among the previously identified genes, transcripts related to chloride channel protein, ecdysone receptor isoform A, fatty acid hydroxylase domain-containing protein 2, pancreatic triacylglycerol lipase, sphingomyelin phosphodiesterase, tribbles homolog 2, and putative inorganic phosphate cotransporter displayed U-shaped patterns along salinity gradients (Fig. 5; Table S7 in Additional File 2). Moreover, genes related to the small heat shock protein ArHsp22, CCAA/enhancer-binding protein, epithelial discoidin domain-containing receptor, PAS domain-containing serine/threonine-

protein kinase, copper-zinc superoxide dismutase, and putative inorganic phosphate cotransporter displayed an inverted U-shaped expression pattern along salinity gradients (Fig. 5; Table S7 in Additional File 2). The gene encoding group 3 late embryogenesis abundant protein, which is down-regulated at high salinities, also showed a U-shaped pattern (Fig. 5; Table S7 in Additional File 2).

Discussion

Halophilic and halotolerant organisms are capable of adapting to high salinity waters and maintaining their internal osmotic balance in order to thrive in harsh environments. In general, the salt-in and salt-out processes are regarded as two distinct osmoregulation strategies. Salt-in organisms typically utilize potassium as the main intracellular cation in high salinity waters, while salt-out organisms accumulate organic solutes (e.g., betaines, glycerol, ectoine, sucrose, and mannitol) as the main osmolytes [17, 59]. In addition, salt-in organisms characteristically contain acidic proteins with a negative charge, which are not observed in the salt-out organisms, to avoid protein aggregation [17, 60]. In the present study, *Artemia* (class Branchiopoda) may be considered a salt-in organism due to increased Na^+/K^+-ATPase activity in high salinity water (230 psu). However, the notable absence of acidic protein profiles in the brine shrimp *Artemia* was identical to other crustaceans in seawater. Thus, our transcriptomic analysis confirms that *A. salina* is a strict hyporegulator [24–26, 61].

In crustaceans, the enzyme Na^+/K^+-ATPase serves to maintain sodium and potassium ion homeostasis across cell membranes [62–65]. Several studies have used the silver staining method to demonstrate that the metepipodites, digestive gut, and maxillary glands in *A. salina* exhibit high Na^+/K^+-ATPase activity under highly saline conditions [24, 26, 61]. This confirms that the enzyme Na^+/K^+-ATPase plays an essential role in *A. salina* osmoregulation at the genetic level. Interestingly, genes related to beta-mannosidase and other enzymes involved with mannose metabolism were up-regulated in high salinity media. This result implies that *A. salina* may accumulate mannose or mannose derivatives as organic osmolytes. Mannose and mannitol are widely recognized as organic osmolytes in diatoms, brown algae, green algae, and terrestrial plants [66, 67]. However, most marine animals accumulate betaine, taurine, trimethylamine oxide, glycine, alanine, proline, homarine, or arginine as organic osmolytes [68]. Thus, the accumulation of mannose and mannose derivatives at high salinities in *A. salina* is particularly interesting. Alternatively, considering that glucose and galactose-related activities were suppressed at high salinities, mannose may be the primary sugar involved in the glycolytic pathway under such conditions. Furthermore, *A. salina* down-regulated UDP-glucose:hexose-1-phosphate uridylyltransferase (synonym: galactose-l-phosphate uridylyltransferase), which converts galactose-1-phosphate into glucose-1-phosphate, at high salinities. This result further supports the theory that mannose is the main energy source used by *A. salina* in highly saline environments. Bunn & Higgins [69] reported that organisms that accumulate high concentrations of aldohexoses with unstable ring structures (i.e., mannose and galactose) may experience enzymatic malfunctions as a result of covalent modifications to individual proteins. Therefore, the covalent modification of *A. salina* proteins may also be detected in high salinity waters. Furthermore, Horst [70] noted that mannose and mannose derivatives in *A. salina* are

substantially involved in glycoprotein catabolic processes, suggesting that exposure to increased salinity may result in an increased activity of mannose-related processes. Investigation of the primary role of mannose and mannose derivatives in *A. salina* under various salinities is warranted.

While *Artemia* can maintain ion homeostasis in its cells as the external salinity increases, more energy is required for growth and reproduction [71]. Theoretically, the dissolved oxygen (DO) concentration in 35 psu media at 25 °C is 3.2 times lower than that in 220 psu media [72]. In this study, we present several pieces of evidence that suggest that low oxygen may substantially impact the growth and reproduction of *A. salina* when salinity increases from 35 psu to 230 psu. Additionally, marine invertebrate vision is one of the most energetically demanding functions and is highly susceptible to dissolved oxygen fluctuations [73]. In high-salinity waters, transcripts related to retinal metabolic processes were significantly up-regulated; *A. salina* significantly up-regulated *ninaB* homologous genes in high-salinity media. Many diverse metazoan species contain *ninaB* homolog genes (Figure S3 in Additional File 3), which are associated with the synthesis of visual pigment and oxidative stress [74–76]. Moreover, the up-regulation of genes related to oxidative stress suggests that *A. salina* can adapt to waters simultaneously high in salinity and low in oxygen. The activity of N-acetylgalactosamine-4-sulfatase, which was one of the down-regulated genes in *A. salina*, can decline when exposed to low oxygen [77]. Therefore, it is likely that the gene expression patterns of *A. salina* are greatly affected by low dissolved oxygen levels in its media.

Few mitochondria and a thin body surface cuticle are characteristic of *Artemia* in low salinity waters, whereas many mitochondria and a thick cuticle have been observed in high salinity waters [23, 27, 54]. In this study, transcripts related to mitochondrion morphogenesis and glycoprotein catabolic processes were up-regulated at high salinities, which is consistent with previous investigations. It is reasonable to infer that the rate of mitochondrion morphogenesis is inversely related to the dissolved oxygen concentration in saline waters. Meanwhile, the increased thickness of the *A. salina* cuticle associated with glycoprotein catabolic processes lowers the water permeability of the body surface, resulting in a relatively low rate of oxygen diffusion [23, 54]. Thus, *A. salina* may require more mitochondria in high salinity than low salinity environments. Most sugar (i.e., glucose and galactose) transport systems, as well as those for nucleotides and amino acids, were repressed in *A. salina* at high salinities. These results imply that *Artemia* may be unable to properly use these essential macromolecules for growth and reproduction under highly saline conditions. Even though *Artemia* spp. are extremely halotolerant and euryhaline, significant energy expenditures are likely required to accommodate these adaptations. However, the increased thickness of *A. salina* body surface layers at high salinities indicates that the reduction in permeability to water, oxygen, and essential nutrients occurs passively. Moreover, several studies have reported decreased protein, carbohydrate, and glycogen contents in some crustacean species with increasing salinity [78–80].

The cellular response of *A. salina* required for acclimation to intermediate salinities depends on the number and type of genes expressed. A U-shaped gene expression pattern observed along the salinity gradient in *A. salina* implies that it can adapt well to intermediate salinities [81, 82], whereas an inverted

U-shaped pattern indicates the presence of salinity response at intermediate salinities [83]. At 150 psu, 411 genes were expressed at low points in U-shaped patterns and only 63 genes were expressed at high points in inverted U-shaped patterns, implying that *A. salina* is well-adapted to 150 psu; most genes were actively expressed to tolerate this salinity. Furthermore, the U-shaped expression patterns observed in *A. salina* represent cellular responses related to cellular signaling, catabolic processes, morphogenesis, and development. Meanwhile, the inverted U-shaped expression patterns were related to diverse environmental response factors (e.g., salt aversion, sensory perception of salty taste, cellular response to light intensity, UV-B, ozone, response to oxidative stress, and starvation). Based on enriched GO terms and KEGG metabolic pathways, the functional annotations of the U-shaped expression pattern genes were usually different from those of the inverted U-shaped expression pattern genes (Fig. 4; Table S6 in Additional File 2; Figure S4 in Additional File 3). This result indicates that the genes related to U-shaped and inverted U-shaped patterns are unequally expressed, and the expression pattern observed at a specific salinity is related to the physiological characteristics of *A. salina*.

Within the genus *Artemia*, the gene expression patterns we observed with increasing salinity were not always consistent with previously identified patterns (Fig. 5; Table S7 in Additional File 2). Intriguingly, the types of genes displaying U-shaped and inverted U-shaped expression patterns were usually differentiated at each intermediate salinity (i.e., 50, 100, and 150 psu). These results demonstrate that *A. salina* could be a potential model organism to study locally adapted populations called 'local adaptation' [19, 84, 85], and differential expression patterns of *Artemia* are likely to fluctuate at the population level. Campillo *et al*. [85] reported that rotifer populations (*Brachionus plicatilis*) might present different cellular responses depending on the salinity of their medium. Thus, the gene expression of *A. salina* could also fluctuate depending on the occurrence of ecological specialization in each population at specific salinities. Further study is needed to confirm that *A. salina* can provide a model for local adaptation.

Conclusions

The gene expression patterns of salt-adapted *A. salina* at five different salinities (35, 50, 100, 150, and 230 psu) displayed greater osmoregulation process complexity than previously thought. *A. salina* along the salinity gradient could differentially express the genes related to the environmental variables (e.g., high salinity and low oxygen) and morphological transformations (e.g., the thickness of the cuticle and the numbers of mitochondria). Moreover, the types of genes displaying U-shaped and inverted U-shaped expression patterns suggested that *A. salina* appeared to have substantially differential adaptive osmoregulatory mechanisms to intermediate salinities.

Abbreviations

IsoSeq
Isoform sequencing; HQ isoform:High-quality isoform; SRA database:Sequence read archive database; ORFs:Open reading frames; BUSCO:Benchmarking universal single-copy orthologs; ML:Maximum likelihood; DEG:Differentially expressed gene; GO:Gene ontology; DO:Dissolved oxygen

Declarations

Ethics approval and consent to participate

Not applicable.

Consent for publication

Not applicable.

Competing interests

The authors declare that they have no competing interests.

Funding

This study was supported by the National Research Foundation of Korea (NRF) grant, funded by the Korea government to JSP (NRF-2019R1A2C2002379), and JML (NRF-2020R1C1C1010193).

Authors' contributions

JSP designed and supervised the transcriptome sequencing project. JML led the transcriptome analysis including transcriptome assembly, phylogenetic analysis, and differentially expressed gene analysis. JML and JSP led the writing of the manuscript. All authors contributed critically to the drafts and gave final approval for publication.

Acknowledgements

We thank Dr. Aaron Heiss at American Museum of Natural History for the valuable comments on the manuscript.

References

1. Javor B. Geology and Chemistry. In: Brock TD, editor. Hypersaline Environments: microbiology and biogeochemistry. Heidelberg: Springer-Verlag; 1989. pp. 5–25.
2. Antón J, Rosselló-Mora R, Rodríguez-Valera F, Amann R. Extremely halophilic bacteria in crystallizer ponds from solar salterns. Appl Environ Microbiol. 2000;66:3052–7.
3. Pedrós-Alió C, Calderón-Paz JI, MacLean MH, Medina G, Marrasé C, Gasol JM, et al. The microbial food web along salinity gradients. FEMS Microbiol Ecol. 2000;32:143–55.

4. Park JS, Choi DH, Hwang CY, Park GJ, Cho BC. Seasonal study on ectoenzyme activities, carbohydrate concentrations, prokaryotic abundance and production in a solar saltern in Korea. Aquat Microb Ecol. 2006;43:153–63.
5. Park JS, Kim H, Choi DH, Cho BC. Active flagellates grazing on prokaryotes in high salinity waters of a solar saltern. Aquat Microb Ecol. 2003;33:173–9.
6. Park JS, Cho BC, Simpson AGB. *Halocafeteria seosinensis* gen. et sp. nov. (Bicosoecida), a halophilic bacterivorous nanoflagellate isolated from a solar saltern. Extremophiles. 2006;10:493–504.
7. Park JS, Simpson AGB, Lee WJ, Cho BC. Ultrastructure and phylogenetic placement within Heterolobosea of the previously unclassified, extremely halophilic heterotrophic flagellate *Pleurostomum flabellatum* (Ruinen 1938). Protist. 2007;158:397–413.
8. Park JS, Simpson AGB, Brown S, Cho BC. Ultrastructure and molecular phylogeny of two heterolobosean amoebae, *Euplaesiobystra hypersalinica* gen. et sp. nov. and *Tulamoeba peronaphora* gen. et sp. nov., isolated from an extremely hypersaline habitat. Protist. 2009;160:265–83.
9. Cho BC, Park JS, Xu K, Choi JK. Morphology and molecular phylogeny of *Trimyema koreanum* n. sp., a ciliate from the hypersaline water of a solar saltern. J Eukaryot Microbiol. 2008;55:417–26.
10. Park JS, Simpson AGB. Characterization of *Pharyngomonas kirbyi* (= "*Macropharyngomonas halophila*" nomen nudum), a very deep-branching, obligately halophilic heterolobosean flagellate. Protist. 2011;162:691–709.
11. Park JS, De Jonckheere JF, Simpson AGB. Characterization of *Selenaion koniopes* n. gen., n. sp., an amoeba that represents a new major lineage within Heterolobosea, isolated from the Wieliczka salt mine. J Eukaryot Microbiol. 2012;59:601–13.
12. Harding T, Brown MW, Plotnikov A, Selivanova E, Park JS, Gunderson JH, et al. Amoeba stages in the deepest branching heteroloboseans, including *Pharyngomonas*: evolutionary and systematic implications. Protist. 2013;164:272–86.
13. Foissner W, Jung JH, Filker S, Rudolph J, Stoeck T. Morphology, ontogenesis and molecular phylogeny of *Platynematum salinarum* nov. spec., a new scuticociliate (Ciliophora, Scuticociliatia) from a solar saltern. Eur J Protistol. 2014;50:174–84.
14. Kirby WA, Tikhonenkov DV, Mylnikov AP, Janouškovec J, Lax G, Simpson AGB. Characterization of *Tulamoeba bucina* n. sp., an extremely halotolerant amoeboflagellate heterolobosean belonging to the *Tulamoeba-Pleurostomum* clade (Tulamoebidae n. fam.). J Eukaryot Microbiol. 2015;62:227–38.
15. Jhin SH, Park JS. A new halophilic heterolobosean flagellate, *Aurem hypersalina* gen. n. et sp. n., closely related to the *Pleurostomum-Tulamoeba* clade: implications for adaptive radiation of halophilic eukaryotes. J Eukaryot Microbiol. 2019;66:221–31.
16. Tikonenkov DV, Jhin SH, Eglit Y, Miller K, Plotnikov A, Simpson AGB, et al. Ecological and evolutionary patterns in the enigmatic protist genus *Percolomonas* (Heterolobosea; Discoba) from diverse habitats. PLoS One. 2019;14:e0216188.

17. Oren A. Organic Compatible Soultes. In: Seckbach J, editor. Halophilic microorganisms and their environments. Dordrecht: Springer; 2002. pp. 279–305.
18. Triantaphyllidis GV, Abatzopoulos TJ, Sorgeloos P. Review of the biogeography of the genus *Artemia* (Crustacea, Anostraca). J Biogeogr. 1998;25:213–26.
19. Gajardo GM, Beardmore JA. The brine shrimp *Artemia*: adapted to critical life conditions. Front Physiol. 2012;3:185.
20. Post FJ, Youssef NN. A procaryotic intracellular symbiont of the Great Salt Lake brine shrimp *Artemia salina* (L.). Can J Microbiol. 1977;23:1232–6.
21. Sung YY, Pineda C, MacRae TH, Sorgeloos P, Bossier P. Exposure of gnotobiotic *Artemia franciscana* larvae to abiotic stress promotes heat shock protein 70 synthesis and enhances resistance to pathogenic *Vibrio campbellii*. Cell Stress Chaperones. 2008;13:59–66.
22. De Vos S, Stappen GV, Sorgeloos P, Vuylsteke M, Rombauts S, Bossier P. Identification of salt stress response genes using the *Artemia* transcriptome. Aquaculture. 2019;500:305–14.
23. Copeland DE. A study of salt secreting cells in the brine shrimp (*Artemia salina*). Protoplasma. 1967;63:363–84.
24. Holliday CW, Roye DB, Roer RD. Salinity-induced changes in branchial Na^+/K^+-ATPase activity and transepithelial potential difference in the brine shrimp *Artemia salina*. J Exp Biol. 1990;151:279–96.
25. Bradley TJ. Animal osmoregulation. New York: Oxford University Press; 2009.
26. Sellami I, Charmantier G, Naceur HB, Kacem A, Lorin-Nebel C. Osmoregulatory performance and immunolocalization of Na^+/K^+-ATPase in the branchiopod *Artemia salina* from the Sebkha of Sidi El Hani (Tunisia). Tissue Cell. 2020;63:101340.
27. Croghan PC. The survival of *Artemia salina* (L.) in various media. J Exp Biol. 1958;35:213–8.
28. Park JS. Effects of different ion compositions on growth of obligately halophilic protozoan *Halocafeteria seosinensis*. Extremophiles. 2012;16:161–4.
29. Li H, Handsaker B, Wysoker A, Fennell T, Ruan J, Homer N, et al. The sequence alignment/map format and SAMtools. Bioinformatics. 2009;25:2078–9.
30. Langmead B, Salzberg SL. Fast gapped-read alignment with Bowtie2. Nat Methods. 2012;9:357–9.
31. Grabherr MG, Haas BJ, Yassour M, Levin JZ, Thompson DA, Amit I, et al. Full-length transcriptome assembly from RNA-Seq data without a reference genome. Nat Biotechnol. 2011;29:644–52.
32. Haas BJ, Papnicolaou A, Yassour M, Grabherr M, Blood PD, Bowden J, et al. *De novo* transcript sequence reconstruction from RNA-Seq: reference generation and analysis with Trinity. Nat Protoc. 2013;8:1494.
33. Patro R, Duggal G, Love MI, Irizarry RA, Kingsford C. Salmon provides fast and bias-aware quantification of transcript expression. Nat Methods. 2017;14:417–9.
34. Tribolium Genome Sequencing Consortium. The genome of the model beetle and pest *Tribolium castaneum*. Nature. 2008;452:949–55.

35. Regier JC, Shultz JW, Zwick A, Hussey A, Ball B, Wetzer R, et al. Arthropod relationships revealed by phylogenomic analysis of nuclear protein-coding sequences. Nature. 2010;463:1079–83.
36. Colbourne JK, Pfrender ME, Gilbert D, Thomas WK, Tucker A, Oakley TH, et al. The ecoresponsive genome of *Daphnia pulex*. Science. 2011;331:555–61.
37. Terrapon N, Li C, Robertson HM, Ji L, Meng X, Booth W, et al. Molecular traces of alternative social organization in a termite genome. Nat Commun. 2014;5:3636.
38. Faddeeva-Vakhrusheva A, Derks MFL, Anvar SY, Agamennone V, Suring W, Smit S, et al. Gene family evolution reflects adaptation to soil environmental stressors in the genome of the collembolan *Orchesella cincta*. Genome Biol Evol. 2016;8:2106–17.
39. Faddeeva-Vakhrusheva A, Kraaijeveld K, Derks MFL, Anvar SY, Agamennone V, Suring W, et al. Coping with living in the soil: the genome of the parthenogenetic springtail *Folsomia candida*. BMC Genom. 2017;18:493.
40. Baldwin-Brown JG, Weeks SC, Long ADA. New standard for crustacean genomes: the highly contiguous, annotated genome assembly of the clam shrimp *Eulimnadia texana* reveals HOX gene order and identifies the sex chromosome. Genome Biol Evol. 2017;10:143–56.
41. Barreto F, Watson ET, Lima TG, Willett CS, Edmands S, Li W, et al. Genomic signatures of mitonuclear coevolution across populations of *Tigriopus californicus*. Nat Ecol Evol. 2018;2:1250–7.
42. Savojardo C, Luchetti A, Martelli PL, Casadio R, Mantovani B. Draft genomes and genomic divergence of two *Lepidurus* tadpole shrimp species (Crustacea, Branchiopoda, Notostraca). Mol Ecol Resour. 2018;19:235–44.
43. Becking T, Chebbi MA, Giraud I, Moumen B, Laverré T, Caubet Y, et al. Sex chromosomes control vertical transmission of feminizing *Wolbachia* symbionts in an isopod. PLOS Biol. 2019;17:e3000438.
44. Lee BY, Choi BS, Kim MS, Park JC, Jeong CB, Han J, et al. The genome of the freshwater water flea *Daphnia magna*: a potential use for freshwater molecular ecotoxicology. Aquat Toxicol. 2019;210:69–84.
45. Zhang X, Yuan J, Sun Y, Li S, Gao Y, Yu Y, et al. Penaeid shrimp genome provides insights into benthic adaptation and frequent molting. Nat Commun. 2019;10:356.
46. Huerta-Cepas J, Forslund K, Coelho LP, Szklarczyk D, Jensen LJ, Von Mering C, et al. Fast genome-wide functional annotation through orthology assignment by eggNOG-mapper. Mol Biol Evol. 2017;34:2115–22.
47. Simão FA, Waterhouse RM, Ioannidis P, Kriventseva EV, Zdobnov EM. BUSCO: assessing genome assembly and annotation completeness with single-copy orthologs. Bioinformatics. 2015;19:3210–2.
48. Waterhouse RM, Seppey M, Simão FA, Manni M, Ioannidis P, Klioutchnikov G, et al. BUSCO applications from quality assessments to gene prediction and phylogenomics. Mol Biol Evol. 2018;35:543–8.

49. Yamada KD, Tomii K, Katoh K. Application of the MAFFT sequence alignment program to large data-reexamination of the usefulness of chained guide trees. Bioinformatics. 2016;32:3246–51.
50. Nguyen LT, Schmidt HA, Von Haeseler A, Minh BQ. IQ-TREE: a fast and effective stochastic algorithm for estimating maximum-likelihood phylogenies. Mol Biol Evol. 2015;32:268–74.
51. Browne RA, Wanigasekera G. Combined effects of salinity and temperature on survival and reproduction of five species of *Artemia*. J Exp Mar Biol Ecol. 2000;244:29–44.
52. Sorgeloos P, Dhert P, Candreva P. Use of the brine shrimp, *Artemia* spp., in marine fish larviculture. Aquaculture. 2001;200:147–59.
53. Jorgensen PL, Amat F. Regulation and function of lysine-substituted Na,K pumps in salt adaptation of *Artemia franciscana*. J Membr Biol. 2008;221:39–49.
54. Mahfouz ME, El-Gamal MM, Shraby SM. Morphology and anatomical structure of the larval salt gland of *Artemia tunisiana* under different salinities. Afr J Biotechnol. 2013;12:6032–41.
55. Zhang Q, Hou M, Li Q, Han L, Yuan Z, Tan J, et al. Expression patterns of As-ClC gene of *Artemia sinica* in early development and under salinity stress. Mol Biol Rep. 2013;40:3655–64.
56. Maniatsi S, Farmaki T, Abatzopoulos TJ. The study of *fkbp* and ubiquitin reveals interesting aspects of *Artemia* stress history. Comp Biochem Physiol B. 2015;186:8–19.
57. Vikas PA, Thomas PC, Sajeshkumar NK, Chakraborty K, Sanil NK, Vijayan KK. Effect of salinity stress on biochemical constituents and ArHsp22 gene expression in *Artemia franciscana*. Indian J Fish. 2016;63:150–6.
58. Zhao W, Yao F, Zhang M, Jing T, Zhang S, Hou L, et al. The potential roles of the G1LEA and G3LEA proteins in early embryo development and in response to low temperature and high salinity in *Artemia sinica*. PLoS One. 2016;11:e0162272.
59. Galinski EA. Osmoadaptation in bacteria. Adv Microb Physiol. 1995;37:273–328.
60. Oren A, Larimer F, Richardson P, Lapidus A, Csonka LN. How to be moderately halophilic with broad salt tolerance: clues from the genome of *Chromohalobacter salexigens*. Extremophiles. 2005;9:275–9.
61. Conte FP. Molecular domains in epithelial salt cell NaCl of crustacean salt gland (*Artemia*). Int Rev Cell Mol Biol. 2008;268:39–57.
62. McNamara JC, Torres AH. Ultracytochemical location of Na^+/K^+-ATPase activity and effect of high salinity acclimation in gill and renal epithelia of the freshwater shrimp *Macrobrachium olfersii* (Crustacea, Decapoda). J Exp Zool. 1999;284:617–28.
63. Thabet R, Ayadi H, Koken M, Leignel V. Homeostatic responses of crustaceans to salinity changes. Hydroboiologia. 2017;799:1–20.
64. Faleiros RO, Garçon DP, Lucena MN, McNamara JC, Leone FA. Short- and long-term salinity challenge, osmoregulatory ability, and (Na^+, K^+)-ATPase kinetics and α-subunit mRNA expression in the gills of the thinstripe hermit crab *Clibanarius symmetricus* (Anomura, Diogenidae). Comp Biochem Physiol Part A Mol Integr Physiol. 2018;225:16–25.

65. Bozza DC, Freire CA, Prodocimo V. Osmo-ionic regulation and carbonic anhydrase, Na^+/K^+-ATPase and V-H^+- ATPase activities in gills of the ancient freshwater crustacean *Aegla schmitti* (Anomura) exposed to high salinities. Comp Biochem Physiol Part A Mol Integr Physiol. 2019;231:201–8.
66. Paul JS. Osmoregulation in the marine diatom *Cylindrotheca fusiformis*. J Phycol. 1979;15:280–4.
67. Wegmann K. Osmoregulation in eukaryotic algae. FEMS Microbiol Rev. 1986;39:37–43.
68. Burg MB, Ferraris JD. Intracellular organic osmolytes: function and regulation. J Biol Chem. 2008;283:7309–13.
69. Bunn HF, Higgins PJ. Reaction of monosaccharides with proteins: possible evolutionary significance. Science. 1981;213:222–4.
70. Horst MN. The biosynthesis of crustacean chitin. Isolation and characterization of polyprenol-linked intermediates from brine shrimp microsomes. Arch Biochem Biophys. 1983;223:254–63.
71. Dana GL, Lenz PH. Effects of increasing salinity on an *Artemia* population from Mono Lake, California. Oecologia. 1986;68:428–36.
72. Sherwood JE, Stagnitti F, Kokkinn MJ, Williams WD. Dissolved oxygen concentrations in hypersaline waters. Limnol Oceanogr. 1991;36:235–50.
73. McCormick LR, Levin LA, Oesch NW. Vision is highly sensitive to oxygen availability in marine invertebrate larvae. J Exp Biol. 2019;222:jeb200899.
74. Arnouk H, Lee H, Zhang R, Chung H, Hunt RC, Jahng WJ. Early biosignature of oxidative stress in the retinal pigment epithelium. J Proteomics. 2011;74:254–61.
75. Jahng WJ. New biomarkers in the retina and RPE under oxidative stress. In: Adio A, editor. Ocular Diseases. Rijeka: INTECH; 2012. pp. 1–36.
76. Poliakov E, Uppal S, Rogozin IB, Gentleman S, Redmond TM. Evolutionary aspects and enzymology of metazoan carotenoid cleavage oxygenases. Biochim Biophys Acta, Mol Cell Biol Lipids. 2020;158665.
77. Bhattacharyya S, Tobacman JK. Hypoxia reduces arylsulfatase B activity and silencing arylsulfatase B replicates and mediates the effects of hypoxia. PLoS One. 2012;7:e33250.
78. Frolov AV, Pankov KN, Geradze KN, Pankova SA. Influence of salinity on the biochemical composition of the rotifer *Brachionus plicatilis* (Muller). aspects of adaptation. Comp Biochem Physiol Part A Mol Integr Physiol. 1991;99:541–50.
79. Verslycke T, Janssen CR. Effects of a changing abiotic environment on the energy metabolism in the estuarine mysid shrimp *Neomysis integer* (Crustacea: Mysidacea). J Exp Mar Biol Ecol. 2002;279:61–72.
80. Anger K. Salinity as key parameter in the larval biology of decapod crustaceans. Invertebr Reprod Dev. 2003;43:29–45.
81. Jensen MK, Madsen SS, Kristiansen K. Osmoregulation and salinity effects on the expression and activity of Na^+, K^+-ATPase in the gills of European sea bass, *Dicentrarchus labra*x (L.). J Exp Zool Part B. 1998;282:290–300.

82. Tine M, Guinand B, Durand JD. Variation in gene expression along a salinity gradient in wild populations of the euryhaline black-chinned tilapia *Sarotherodon melanotheron*. J Fish Biol. 2012;80:785–801.
83. Jeffries KM, Fangue NA, Connon RE. Multiple sub-lethal thresholds for cellular responses to thermal stressors in an estuarine fish. Comp Biochem Physiol Part A Mol Integr Physiol. 2018;225:33–45.
84. Gajardo GM, Abatzopoulos TJ, Kappas I, Beardmore JA. Evolution and speciation. In: Abatzopoulos TJ, Beardmore JA, Clegg JS, Sorgeloos P, editors. Artemia: basic and applied biology. Dordrecht: Springer; 2002. pp. 225–50.
85. Campillo S, García-Roger EM, Carmona MJ, Serra M. Local adaptation in rotifer populations. Evol Ecol. 2011;25:933–47.

Figures

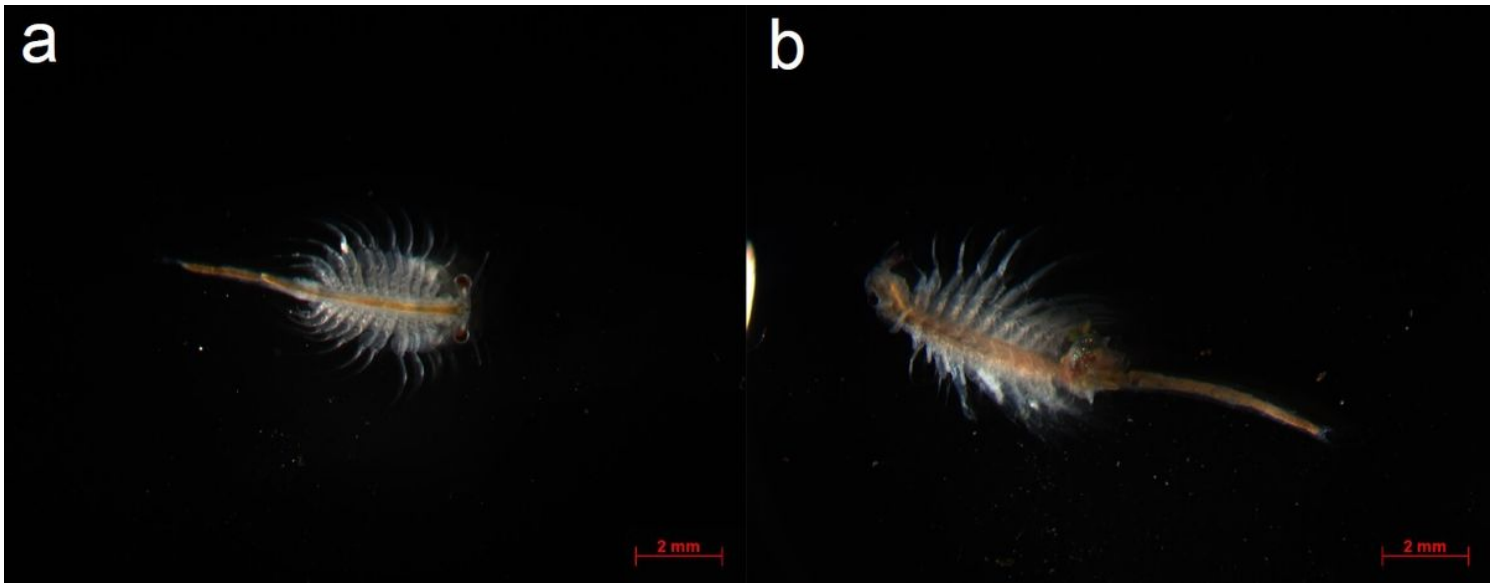

Figure 1

Photographs of a) male and b) female Artemia salina specimens from present study.

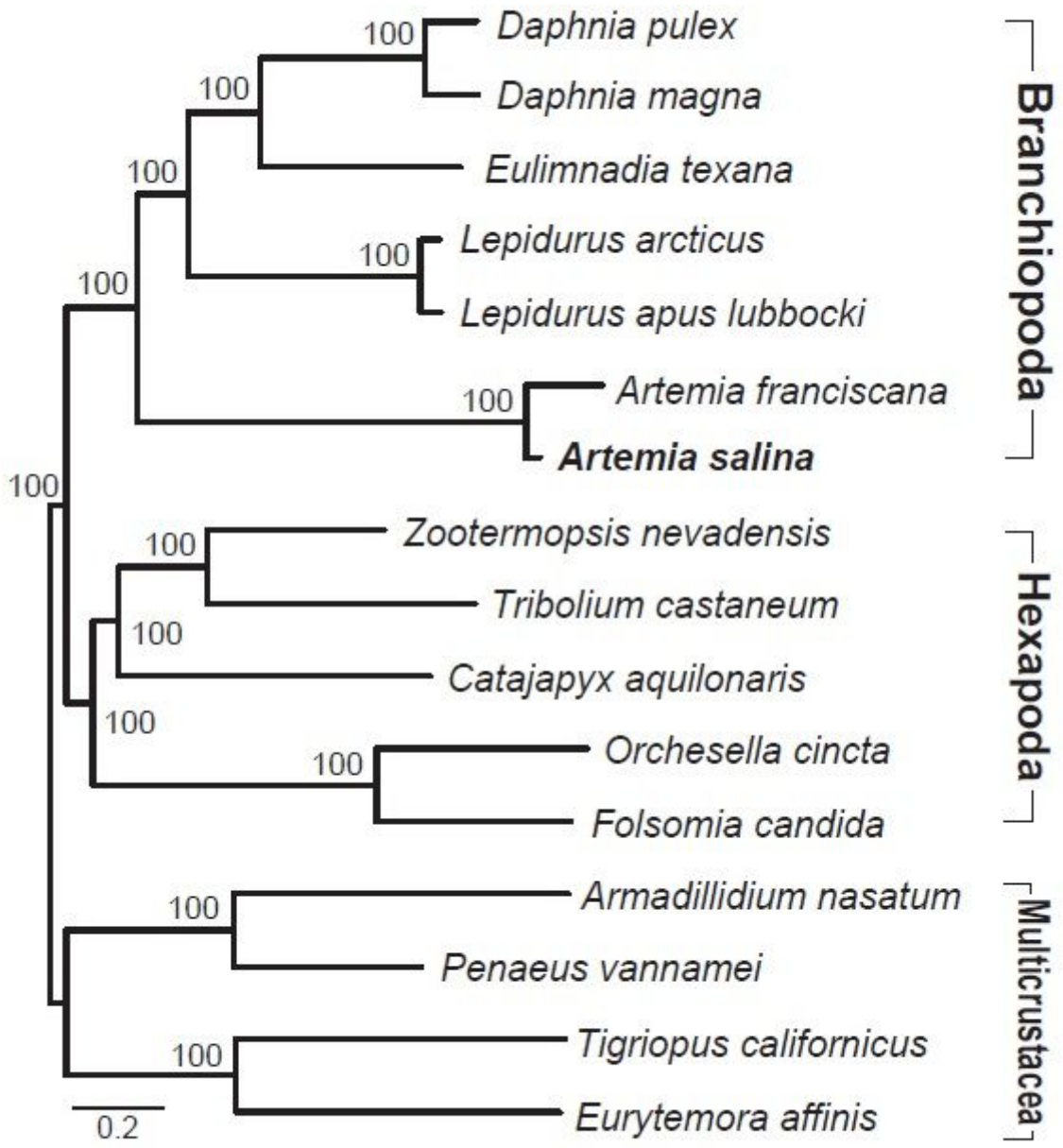

Figure 2

Phylogenetic tree of Pancrustacea. A total of 5,604 homologous protein sets were present in all sampled Branchiopoda species.

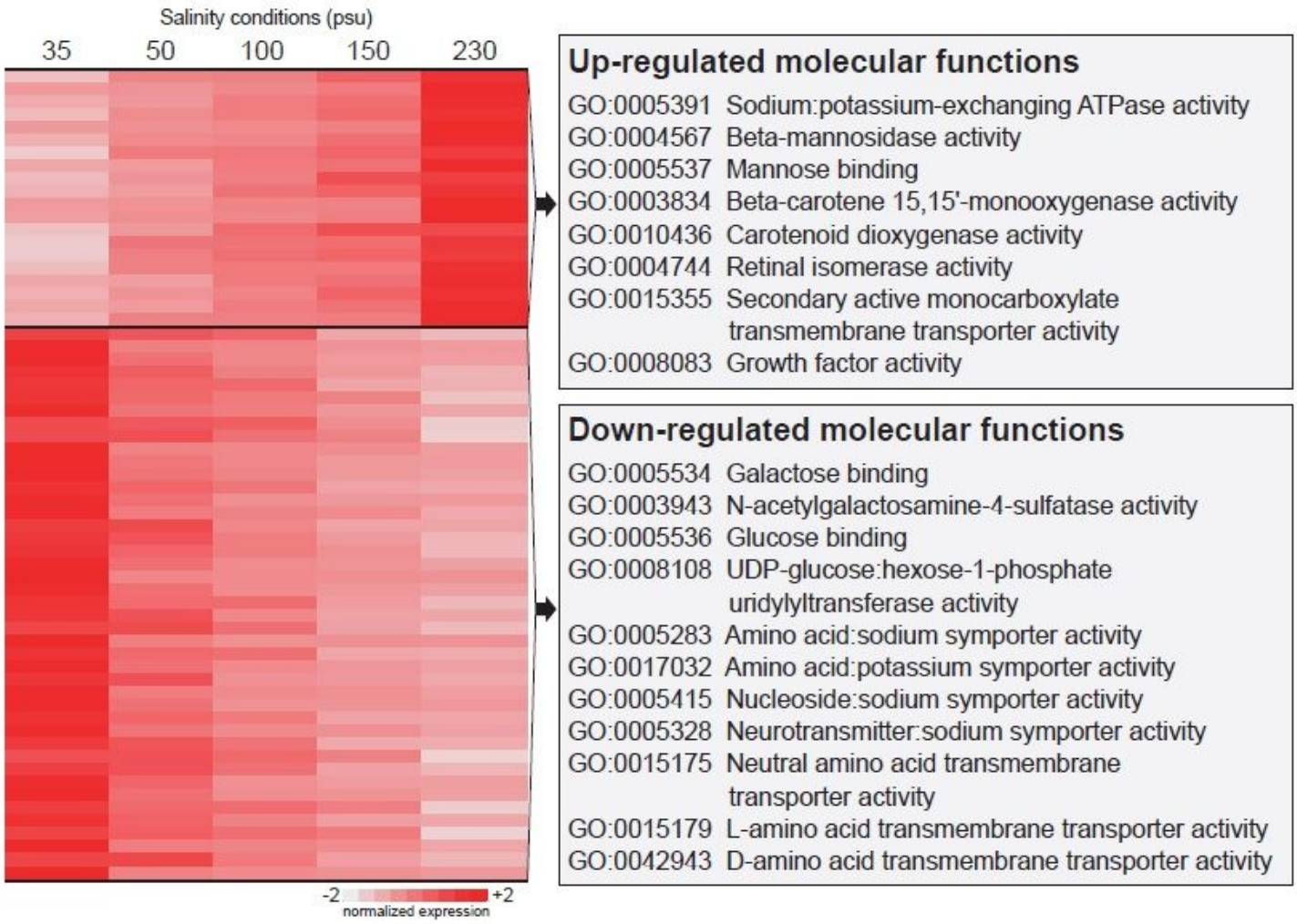

Figure 3

Heatmap of expression patterns of up- and down-regulated genes with increasing salinity from 35 psu to 230 psu. Normalized expressions indicate z-scores. Molecular functions of enriched gene ontology terms are shown (Fisher test, p-value < 0.05).

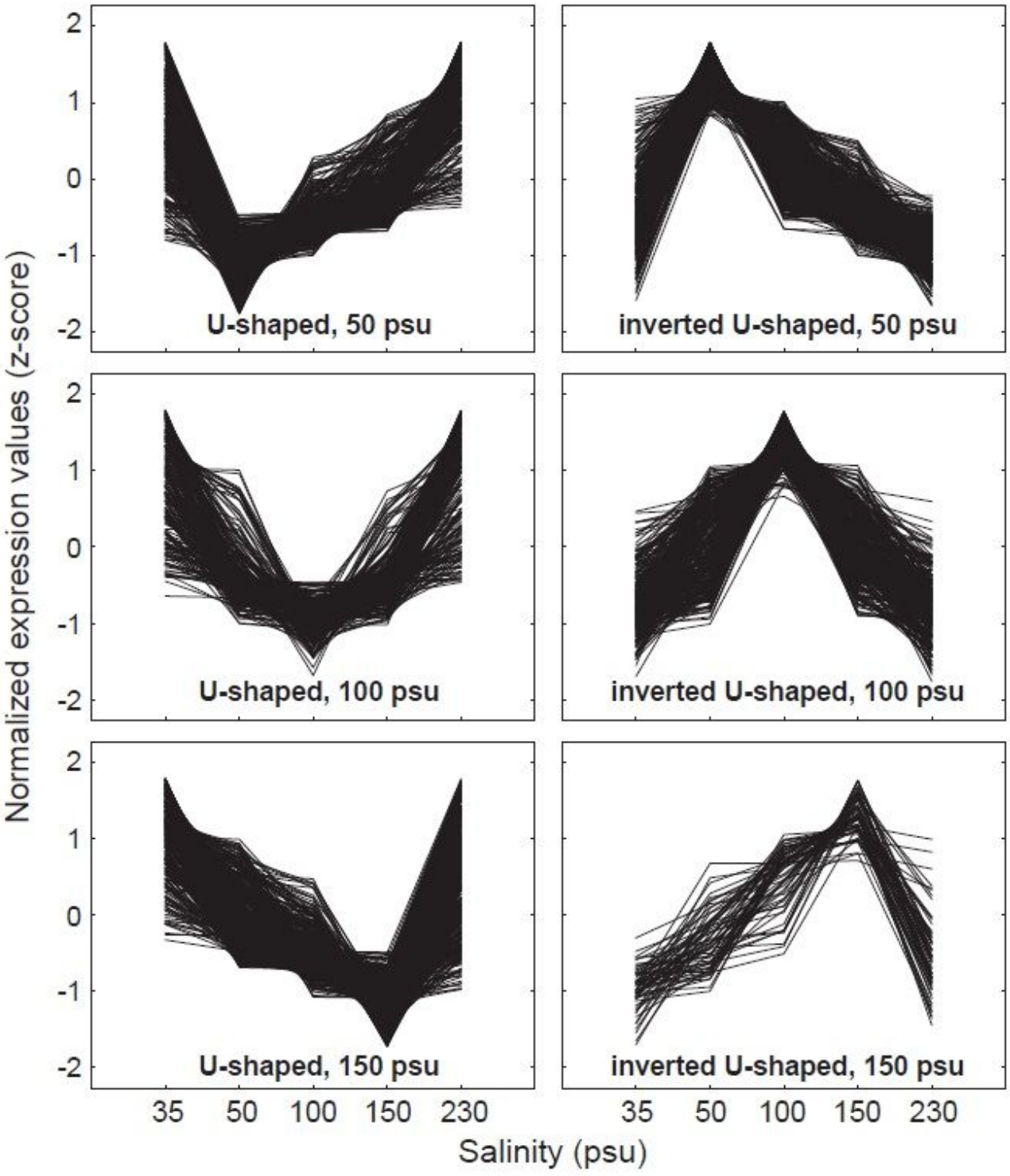

Figure 4

Hypothetical U-shaped and inverted U-shaped responses with increasing salinity from 35 psu to 230 psu. Normalized values (z-scores) were used to identify the U-shaped or inverted U-shaped patterns.

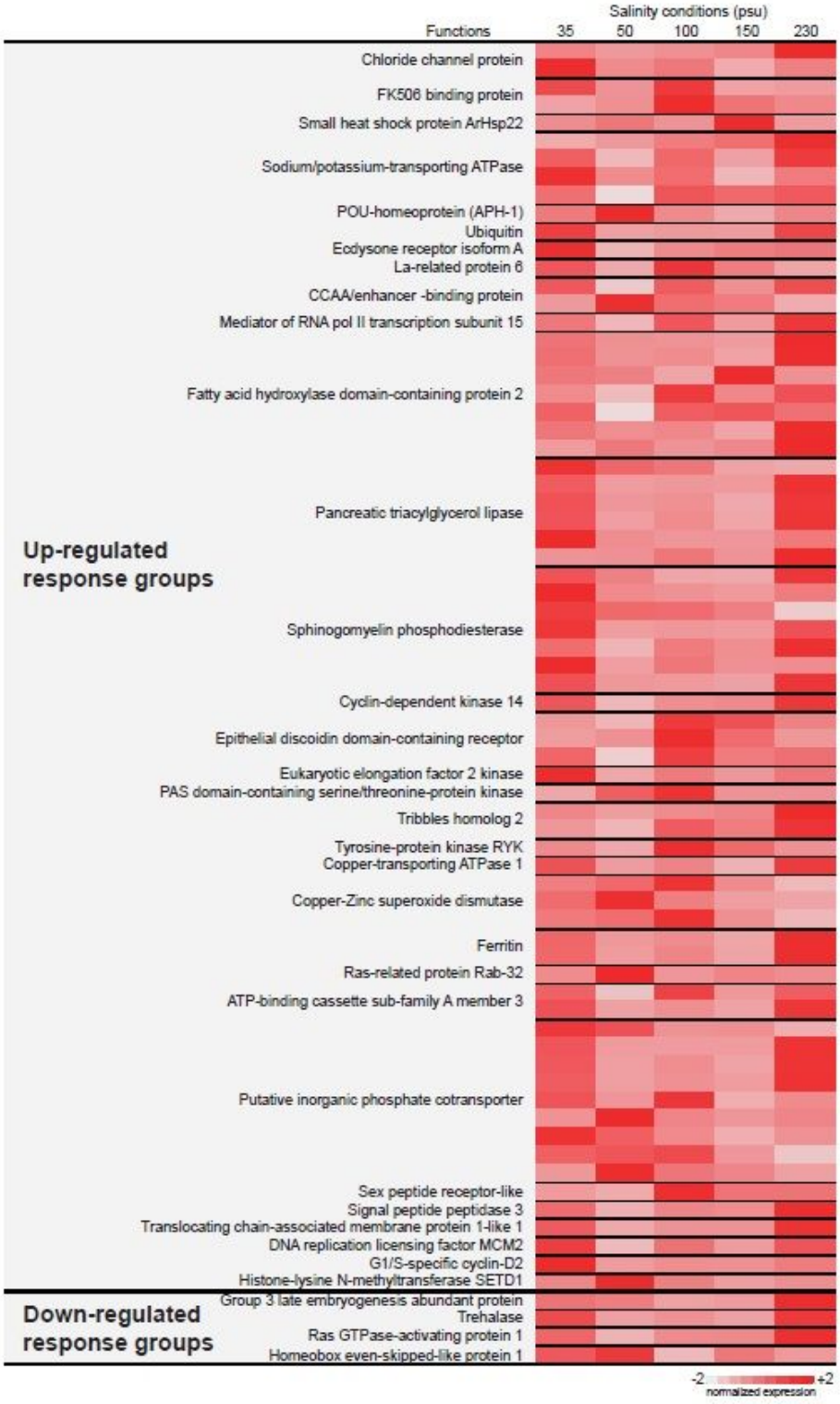

Figure 5

Comparative analysis of Artemia salina gene expressions with previously identified salinity-dependent up- and down-regulated response genes. Normalized expressions indicate z-scores.

Supplementary Files

This is a list of supplementary files associated with this preprint. Click to download.

- Additionalfile1.mp4
- Additionalfile2.xlsx
- Additionalfile3.pdf
- Additionalfile4.xlsx